Colloids and Surfaces B: Biointerfaces 73 (2009) 229–236

Contents lists available at ScienceDirect

Colloids and Surfaces B: Biointerfaces

journal homepage: www.elsevier.com/locate/colsurfb

Non-specific adhesion on biomaterial surfaces driven by small amounts of protein adsorption

Surachate Kalasin[a], Maria M. Santore[b,*]

[a] Department of Physics, University of Massachusetts, 120 Governors Drive, Amherst, MA 01003, USA
[b] Department of Polymer Science and Engineering, University of Massachusetts, 120 Governors Drive, Amherst, MA 01003, USA

ARTICLE INFO

Article history:
Received 3 February 2009
Received in revised form 5 May 2009
Accepted 25 May 2009
Available online 6 June 2009

Keywords:
Bioadhesion
Bacterial adhesion
Flow
Biofouling
Electrostatic
Salt effects
Screening
Heterogeneity
Hydration effects
Charge patchiness

ABSTRACT

This work explores how long-range non-specific interactions, resulting from small amounts of adsorbed fibrinogen, potentially influence bioadhesion. Such non-specific interactions between protein adsorbed on a biomaterial and approaching cells or bacteria may complement or even dominate ligand–receptor mating. This work considers situations where the biomaterial surface and the approaching model cells (micron-scale silica particles) exhibit strong electrostatic repulsion, as may be the case in diagnostics and lab-on-chip applications. We report that adsorbed fibrinogen levels near 0.5 mg/m^2 produce non-specific fouling. For underlying surfaces that are less fundamentally repulsive, smaller amounts of adsorbed fibrinogen would have a similar effect. Additionally, it was observed that particle adhesion engages sharply and only above a threshold loading of fibrinogen on the collector. Also, in the range of ionic strength, *I*, below about 0.05 M, increases in *I* reduce the fibrinogen needed for microparticle capture, due to screening of electrostatic repulsions. Surprisingly, however, ionic strengths of 0.15 M reduce fibrinogen adsorption altogether. This observation opposes expectations based on DLVO arguments, pointing to localized electrostatic attractions and hydration effects to drive silica–fibrinogen adhesion. These behaviors are benchmarked against microparticle binding on silica surfaces carrying small amounts of a polycation, to provide insight into the role of electrostatics in fibrinogen-driven non-specific adhesion.

1. Introduction

Protein adsorption is universally considered to be the precursor to cell adhesion, driving an enormous scientific focus on the tendency of biomaterials to adsorb these complex and varied molecules. The adsorption of proteins from solutions such as serum mediates cell adhesion, including platelet activation and leukocyte binding in the clotting and inflammation cascades, respectively. Of particular current interest, driven by growing bacterial resistance to antibiotics, are factors which influence bacterial adhesion. A number of adsorbed proteins enable the specific binding of *Staphylococcus aureus*, for instance, fibronectin [1–6], fibrinogen [1,7–9], vitronectin [10,11], thrombospondin [12], and Von Willebrand factor [13]. In some cases, the specific bacterial adhesin which binds these proteins is known: clumping factor A binds fibrinogen [14,15].

Cellular and bacterial recognition of specific proteins adsorbed on a biomaterial is typically thought to be short-range, involving the close approach of complementary molecules [16–20]. When cells interact with protein-coated biomaterials, the ligands and receptors are influenced and potentially dominated by a background field of electrostatic, hydrogen bonding, steric, and hydrophobic interactions [21,22]. In the extreme, there may be cases where long-range repulsions prevent the close approach necessary for receptor mating [23,24]. Likewise, if the non-specific interactions are attractive, cell adhesion may occur without ligand–receptor interactions [25–28]. Indeed this occurs sufficiently frequently that enormous effort has been invested in the development of fouling-resistant surfaces, with biocompatibility often gauged by the extent of protein adsorption [29–33]. In order to anticipate bio-fouling and to predict conditions that broadly lead to colonization by bacteria or adhesion by other cells, an understanding of non-specific interactions is critical. Of particular interest is how non-specific adhesion from adsorbed proteins influences specific binding, and how much of these non-specific attractions might be needed to capture cells or bacteria, defeating a bio-resistant coating.

This paper focuses on the non-specific aspects of biomaterial interactions to provide insight into when cell/bacterial adhesion may occur without receptor engagement. The study also addresses, indirectly, the conditions that can prevent specific cell–substrate adhesion. Fibrinogen is chosen as a model biomaterial "contaminant", and the study examines how fibrinogen alters the interfacial environment before specific interactions are considered. Fibrinogen is chosen because of its ubiquity in different biomaterial applications. Indeed, fibrinogen has been shown to be the most universally

* Corresponding author.
E-mail address: santore@mail.pse.umass.edu (M.M. Santore).

0927-7765/$ – see front matter © 2009 Elsevier B.V. All rights reserved.
doi:10.1016/j.colsurfb.2009.05.028

adsorbing protein in applications such hemodialysis [7] and can be responsible for infections of heart valves by *S. aureus* [34]. Fibrinogen is negatively charged but contains substantial hydrophobic and cationic functionality [35–37].

This study starts with surfaces that are fundamentally electrostatically repulsive: micron-sized silica particles and planar silica flats. Fibrinogen is added to the planar surface in small amounts, and the adhesion of the negative microparticles is studied as a function of the amount of fibrinogen on the flat. Variations in ionic strength tune the range and strength of the background repulsion providing insight into the nature of the fibrinogen-driven attractions: though fibrinogen is net negative, its small positive domains may contribute electrostatic attractions, while hydrophobic and hydrogen-bonding interactions may also be important.

Also worth noting, the choice of silica microparticles as "model cells" serves two purposes. First, they are strongly electrostatically repulsive towards the silica substrate prior to its fouling. Therefore, the fibrinogen levels reported here are an upper bound on the amount of protein adsorption which can be tolerated prior to non-specific cell capture. If the particles were less fundamentally repulsive toward the substrate, lower doses of fibrinogen would enable their capture. Second, the silica microparticles comprise a useful benchmark for *S. aureus* bacteria, which are also 1 μm spheres of fairly dense negative charge, with zeta potentials near −30 mV [38,39], though differences arise from the brushy surface nature of some strains [40]. Indeed, we have previously demonstrated parallel behavior between the capture of these silica particles in flow on electrostatically patchy surfaces and the capture of *S. aureus* on collagen-containing surfaces [41,42]. A well-characterized benchmark, such as silica particles, facilitates an understanding of factors such as charge heterogeneity, known to influence bacterial adhesion [43,44].

This study identifies a minimum surface loading of fibrinogen that produces non-specific capture of the negative silica microparticles. Interestingly, the microparticle adhesion develops relatively sharply with increasing fibrinogen contamination, but does not occur at all below a threshold. This work interprets the threshold in terms of the arrangement of fibrinogen on the substrate. The relative roles of electrostatic and other (hydrophobic/hydrogen bonding) attractions are evaluated by parallel experiments where a cationic polymer is used as a model biomaterial foulant.

2. Materials and methods

Bovine plasma fibrinogen IV, from Sigma (95% clottable), was used without further purification. Salts for phosphate buffer solutions, Na_2HPO_4, KH_2PO_4, and NaCl were purchased from Fisher Scientific. The main component of the pH 7.4 buffer was a mixture of 0.008 M Na_2HPO_4 and 0.002 M KH_2PO_4 which produced a solution having an ionic strength of 0.026 M. Dilution of this buffer to an ionic strength of 0.005 M did not appreciably alter the pH. Physiological buffer was made by adding 0.15 M NaCl to the 0.026 M phosphate buffer to produce a solution having an ionic strength of 0.176 M.

Fisherfinest (Fisher Scientific) microscope slides were employed as substrates. These were soaked in concentrated sulfuric acid overnight, and then rinsed in substantial amounts of DI (deionized) water. The purpose of this treatment was to remove Na^+, Ca^{2+}, K^+ and similar cations from the near-surface region to produce silica substrates more nearly similar to those of the silica spheres [35,45].

All fibrinogen adsorption onto silica substrates was conducted in a shear flow cell [46,47] at a wall shear rate of 25 s^{-1}, from a bulk solution concentration of 25 ppm in 0.026 M phosphate buffer, unless specifically noted. These fixed conditions for fibrinogen adsorption were applied throughout the study so that the initial adsorbed fibrinogen configurations were as uniform as possible, even though particle adhesion was studied at different ionic strengths. When less than a fully saturated layer of fibrinogen was desired, the fibrinogen was flowed for a controlled amount of time and then the bulk solution was switched back to 0.026 M buffer to halt the growing coverage. We previously demonstrated that the adsorbed amount of fibrinogen on silica could be precisely controlled in this fashion, based on the timing of the flowing fibrinogen solution, and not requiring on-line monitoring of the fibrinogen accumulation [35,48].

1 μm diameter silica spheres were purchased from GelTech (Orlando), while 0.5 μm diameter silica spheres were purchased from Fiber Optic Center, Inc. (New Bedford, MA). Adhesion of these particles onto fibrinogen-containing surfaces from flowing suspension was studied in the same slit-shear cell employed for fibrinogen adsorption. The flow chamber was oriented perpendicular to the floor so that gravity did not affect particle–surface interactions.

In experiments where fibrinogen adsorption was monitored, near-Brewster optical reflectometry was typically used because particle adhesion could subsequently be monitored. Control runs demonstrating fibrinogen retention on the substrate during exposure to particle flow required total internal reflectance fluorescence (TIRF). TIRF employs fibrinogen labeled with fluorescein isothiocyanate (FITC) from Sigma. We chose TIRF for these control studies because it gives a clear interpretation of the fibrinogen level in the presence of adherent particles. Fibrinogen labeling was conducted at room temperature in carbonate buffer, and purification was done using a Biogel P-6 gel column, as previously detailed [47,49]. When labeling is accomplished at levels of three per protein or less, as was the case here, TIRF provides an unambiguous measure of the amount of adsorbed protein [47,49].

Near-Brewster optical reflectometry can monitor protein adsorption and particle deposition in series [50,51]. (Measuring protein adsorption prior to particle adhesion is not always necessary, as proteins can be adsorbed precisely in a blind fashion [35].) Our instrument, described previously in detail [52], employs a 633 nm HeNe laser. For small silica particles and adsorbing proteins, the square root of the reflectance is linear in adherent particle mass [50,52]. For the 1 μm particles, however, the square root of the reflectance requires calibration relative to transport-limited particle deposition [51]. In the current study, some of the data for particle deposition have been obtained with reflectometry, while some data were obtained with video-microscopy (a new instrument built part-way into our program). The latter is more direct, and easier to use but cannot be used to track fibrinogen adsorption preceding particle capture. When video-microscopy was employed to monitor particle deposition, it was done in a home-built lateral microscope, employing a 20× objective [41,53].

Studies assessing the contribution of electrostatic attractions to the adhesive nature of fibrinogen employed a sample of polydimethylaminoethyl methacrylate (pDMAEMA) from DuPont. It was 31,300 molecular weight and monodisperse. As described previously [41,50,51,54–57] it was transferred from alcohol to aqueous solution and then to the desired buffer. pDMAEMA was adsorbed sparsely to acid-etch silica from a 20 ppm solution in a slit-shear flow cell at a wall shear rate of 5 s^{-1}, with conditions for small levels of adsorption being well established. Our prior studies demonstrate that adsorbed pDMAEMA layers are retained completely below pH 8 [56–58] and that adsorbed chains also tends to lie flat on the surface [55]. The current study focuses mostly on situations involving isolated adsorbed pDMAEMA coils.

Measurement of zeta potentials employed 1 μm silica particles with different levels of adsorbed fibrinogen or pDMAEMA to assess the electrostatic conditions at the planar surfaces in the particle adhesion studies. (Since the curvature of the 1 μm particles is large compared with the dimensions of the adsorbing molecules, these

zeta potentials are expected to reasonably estimate those of the planar surfaces.) Protein or polymer solutions were mixed with dilute silica suspensions and incubated for sufficient time, typically overnight, that all the protein or polymer molecules could adsorb. (This was done for proportions such that the surfaces tended to be unsaturated, as was the case for the planar surfaces.) Adsorption was considered complete when longer incubation periods did not affect the zeta potential. Zeta potentials were measured on a Malvern Zetasizer Nano ZS instrument. Five separate runs were averaged at each concentration and data were checked to ensure that only a single sharp peak was present in each sample, indicating a single population.

3. Results and discussion

3.1. Adsorption of fibrinogen and characterization of Fb-containing surfaces

Fig. 1 shows the kinetic traces via TIRF for fibrinogen adsorption. Part A shows the runs conducted in buffers of different ionic strengths while Part B shows adsorption from $I = 0.026$ M buffer, followed by a change in conditions. Part A demonstrates that there is a substantial impact of ionic strength on the ultimate adsorbed amount of fibrinogen on silica, with the saturation coverage reduced as ionic strength is increased. This suggests that while there may be several factors contributing to the driving force for fibrinogen adsorption, electrostatic attractions between positively charge protein domains and negative silica become screened: at high ionic strength the driving force is dominated by other factors. Also in Fig. 1A, all the layers are retained when the bulk solution is switched back to a buffer having the same ionic strength as the adsorbing protein solution.

Because of the lower fibrinogen coverages at the higher ionic strengths, and our desire to fix the adsorbed fibrinogen conformation by conducting all fibrinogen deposition at the same ionic strength, we had to take care concerning the history for the fibrinogen adsorption runs relative to the conditions for the study of particle adhesion. Specifically, since fibrinogen was always adsorbed at $I = 0.026$ M, we needed to establish what would happen to the fibrinogen layer if the ionic strength were increased after fibrinogen adsorption.

Fig. 1B more closely approximates the protein adsorption protocols used in silica particle adhesion studies. Here, in run (i) fibrinogen is adsorbed from an $I = 0.026$ M phosphate buffer solution to saturation. In run (ii) $I = 0.026$ M buffer is re-injected before saturation to limit the adsorbed amount to give a lower coverage. In runs (i) and (ii), after the bulk solution is replaced with flowing 0.026 M phosphate buffer, both layers are retained, consistent with Fig. 1A. When the 0.026 M buffer is subsequently switched to $I = 0.176$ M buffer, however, the coverage decreases. In run (i), for a fully saturated fibrinogen layer, the adsorbed amount drops from about 4 to 2 mg/m^2 after the increase in ionic strength. Here the ultimate coverage is in good agreement with the run in Fig. 1A where the fibrinogen was adsorbed directly from 0.176 M buffer. In run (ii), the coverage is reduced in the unsaturated layer when buffer is re-injected. This suggests that even with limited levels of adsorbed fibrinogen, increases in ionic strength will remove some protein, introducing uncertainty into our particle deposition studies.

Because of the importance of establishing fibrinogen retention and knowing the amount of fibrinogen on the surface, we omitted adhesion experiments in 0.176 M buffer that did not involve fully saturated layers. We further confirmed, but do not show here, that fully saturated and partial layers of fibrinogen adsorbed from $I = 0.026$ M buffer are retained in buffers of lower ionic strength, as Fig. 1A would suggest. Also, we employed TIRF experiments with fluorescently tagged fibrinogen to establish that the fibrinogen coverage was not altered by flowing silica particles in the particle adhesion portions of the investigation. Finally, the inset of Fig. 1B shows the highly reproducible initial adsorption kinetics of these fibrinogen runs, allowing us to load controlled amounts of fibrinogen on the surface based on the timing of buffer re-injection.

Fig. 2 provides further perspective on the average electrostatic nature of fibrinogen-containing silica surfaces. Shown here are the zeta potentials of 1 μm particles carrying different amounts of adsorbed fibrinogen, at the ionic strengths indicated. As zeta potential measurement requires a particulate substrate, the 1 μm particles we had on-hand for the particle deposition experiments turned out to be convenient for these characterization studies. The y-axis of Fig. 2 illustrates that the zeta potential of the underlying bare silica surface becomes less negative with increasing ionic strength, as expected. This is due primarily to the compression of

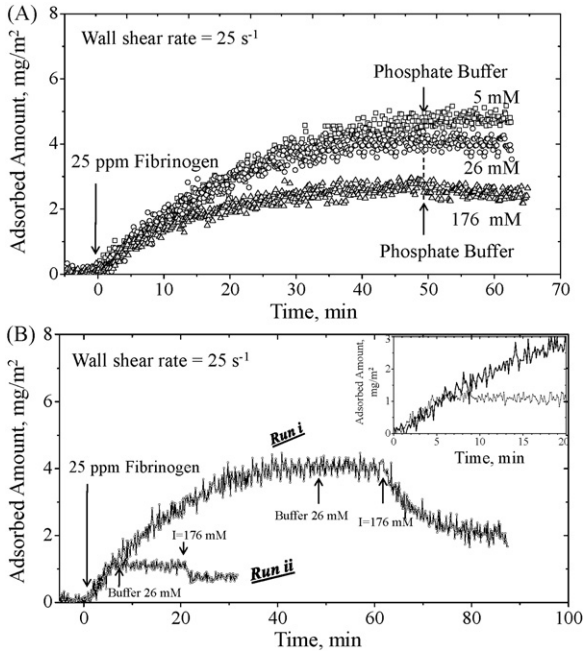

Fig. 1. (A) FITC-tagged fibrinogen adsorption on silica from buffers of three different ionic strengths, measured via TIRF. Arrow shows the time at which phosphate buffer, of the same ionic strength as during adsorption, was re-injected for all three runs, flushing the fibrinogen from the fluid space. (B) Adsorption of fibrinogen (25 ppm) from $I = 0.026$ M phosphate buffer at a wall shear rate of 25 s^{-1}. After adsorption, 0.026 M phosphate buffer is re-injected, followed about 10 min later by 0.176 M phosphate-buffered saline. The inset highlights the reproducibility of the initial kinetics.

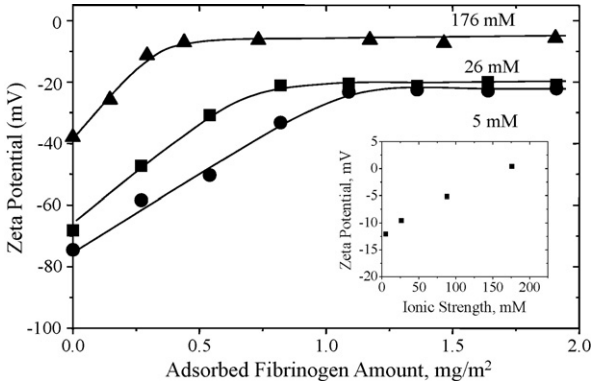

Fig. 2. Zeta potentials of fibrinogen adsorbed onto 1-μm silica particles at three different ionic strengths. The inset shows the zeta potential of fibrinogen in free solution as a function of ionic strength. Curves have been drawn to guide the eye.

the double layer with added salt, while the position of the shear plane is relatively uninfluenced by the additional salt. Additionally, as pointed out by a reviewer, there may be some specific ion adsorption; however, our zeta potential data cannot determine if ion adsorption is taking place. As fibrinogen is added to the surface, in all cases, the magnitude of the zeta potential is also reduced and ultimately levels off at values close to the zeta potential of fibrinogen in free solution (shown in the inset), for each ionic strength.

The most important feature of Fig. 2, relevant to the particle adhesion studies, is that regardless of the fibrinogen loading on the silica, the average electrostatic character of the surfaces is net negative and would be expected to repel approaching negative microparticles (and cells/bacteria), from a purely mean-field perspective. There are no conditions where the average surface character is net positively charged. This is consistent with zeta potentials of the fibrinogen molecules themselves: while different parts of the 47-nm long molecule have different local charge (for instance the net positive character of the central e-domain [36]), the overall charge on fibrinogen at pH 7.4 is negative. As fibrinogen is, overall, less negative than the silica surface to which it adsorbs, the zeta potential of silica with adsorbed fibrinogen is less negative than that of bare silica. Further, since fibrinogen and silica are both net negative, there is an overall repulsion working against fibrinogen adsorption; however, the localized interactions between positive fibrinogen domains and the silica may favor adsorption, along with hydrogen bonding and other interactions, especially those involving the water structure around silica and around the protein itself. Release of bound water will strongly favor adsorption by increasing the overall translational entropy.

Fig. 2 also illustrates that in $I = 0.176$ M phosphate-buffered saline, fibrinogen is nearly neutral, as opposed to being negative at lower ionic strength. This observation makes the impact of $I = 0.176$ M phosphate buffer on fibrinogen adsorption, in Fig. 1, surprising if one assumes that average electrostatic forces dominate. The combination of Figs. 1 and 2 therefore emphasizes the importance of local interactions in driving silica–fibrinogen interactions.

Fig. 3A illustrates the adsorption of pDMAEMA on silica, to be contrasted with fibrinogen adsorption in Fig. 1A in the same buffers. Here, the saturated adsorbed amount, 0.35–0.55 mg/m^2, of this polycation is small relative to saturated fibrinogen coverage, consistent with the lower 31,300 molecular weight of pDMAEMA relative to the 340,000 molecular weight of fibrinogen. While increased ionic strength slightly reduces the saturation coverage of pDMAEMA layers, the layers are each well-retained when buffer of the same ionic strength as used during adsorption is re-injected. This slight reduction in pDMAEMA coverage with increasing ionic strength is explained by screening of electrostatic attractions between the substrate and polymer chains, which is well-established [59]. In Fig. 3B, which is a similar plot to Fig. 1B, pDMAEMA layers, originally adsorbed in $I = 0.026$ M buffer are well-retained when the ionic strength is increased. This cannot be seen directly in the reflectometry runs of Fig. 1B: when the higher ionic strength buffer is injected, the signal quickly rises due to bulk solution refractive index changes; however, when the original 0.026 M buffer is re-injected, the signal recovers its original level, indicating retention of the polymer layer. This is the case in run (i) with a saturated pDMAMEA layer, and also in run (ii) with a partial pDMAEMA layer whose coverage has been limited by re-injection of the 0.026 M buffer prior to saturation.

Fig. 4, which contains zeta potential data analogous to Fig. 2 for pDMAEMA on silica, illustrates that the composite surfaces possess a net negative charge as long as the adsorbed amount is below about 0.2–0.3 mg/m^2, depending on ionic strength. At higher coverages, the surface can become slightly positively charged, though this is beyond the range of coverages relevant in the particle adhesion studies to follow. The average electrostatic character of these surfaces results from the net positive charge of the pDMAEMA and the relatively greater densities of the positive charge on the pDMAEMA compared to the negative charge density on the silica at this pH [54].

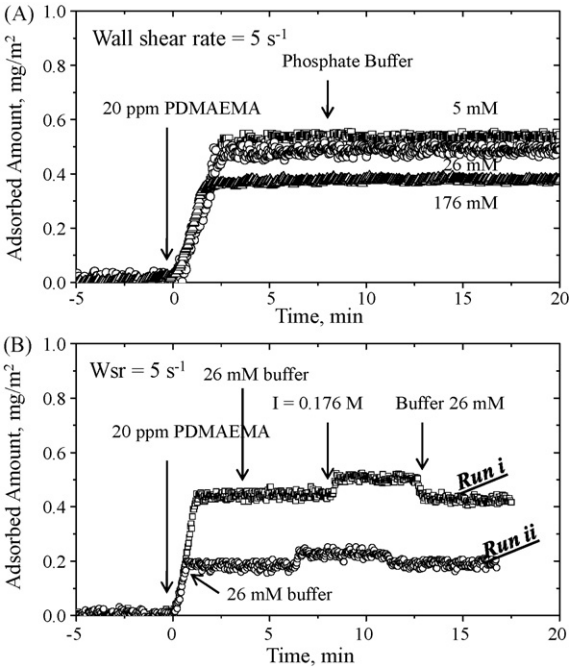

Fig. 3. Kinetic traces of pDMAEMA adsorption at a wall shear rate of 5 s^{-1}. (A) From buffers of three different ionic strengths with re-injection of the same buffer after layer saturation. (B) From $I = 0.026$ M buffer, followed by re-injection of $I = 0.026$ M buffer, then $I = 0.2$ M buffer, and then 0.026 M buffer.

3.2. Silica particle adhesion on fibrinogen-containing surfaces

Fig. 5 shows example particle deposition rate traces for 1 μm silica particles adhering from flowing suspension (25 s^{-1}) onto silica surfaces carrying different levels of fibrinogen, for phosphate buffers having ionic strengths of 0.005 and 0.026 M. The data are linear in time for the first 10 min, as shown here, and often for much longer times (order 100 min), with the slope strongly dependent on the amount of adsorbed fibrinogen. The linearity of these curves suggests that particle adhesion at any particular instant is controlled by the nature of the underlying surface in most cases (or by transport considerations when the particle–surface attractions are sufficiently strong that the intrinsic particle capture rate is rapid), not by the amount of particles deposited prior to the instant of

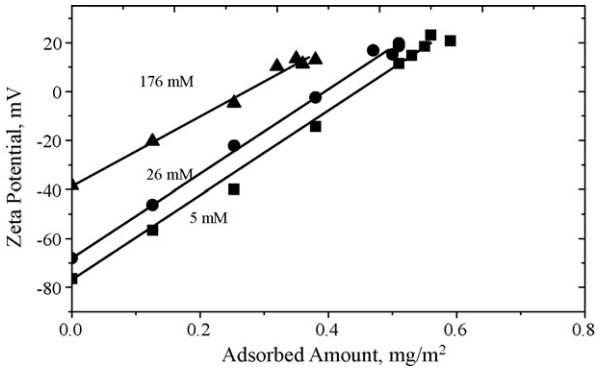

Fig. 4. Zeta potentials of pDMAEMA adsorbed onto 1-μm silica particles at three different ionic strengths. Lines have been drawn to guide the eye. Conditions are for pH 7.4.

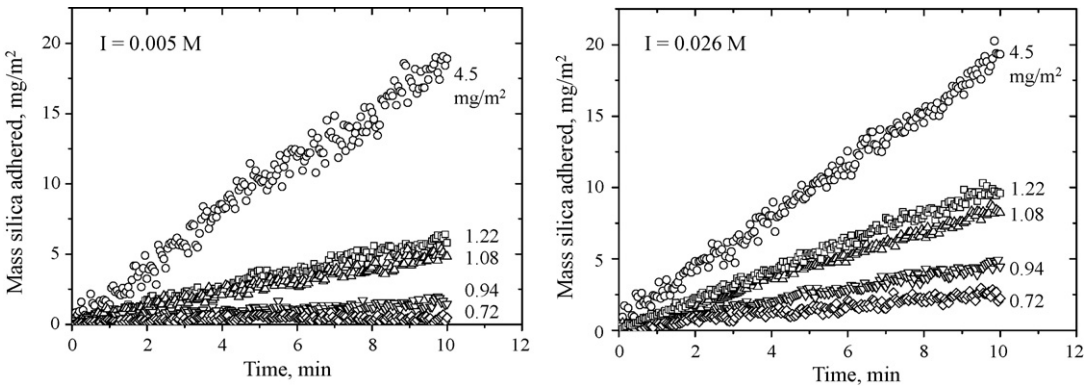

Fig. 5. Amount of silica microspheres adhering to fibrinogen-containing silica flats in 5 and 26 mM, phosphate buffer. The fibrinogen surface loading is indicated on each curve.

interest. Hence the particle deposition rates reflect the interactions of single silica particles with the substrate.

The rate data of Fig. 5, along with other similar runs, are summarized in Fig. 6, which plots the *rate* of particle capture as a function of the loading of fibrinogen (or pDMAEMA) on the silica flat. The two rightmost data sets of Fig. 6A are for fibrinogen on the silica flat for buffer ionic strengths of 0.005 and 0.026 M. The data are quite reproducible so that the features of the curves, including the crossing of the data sets at a single point are meaningful. Indeed a detailed analysis of this form of data for particle capture on heterogeneous surfaces has recently been developed [53]. These data exhibit several important features. First, at high fibrinogen coverages of about 1.6 mg/m^2 or greater (saturated fibrinogen coverage is 4 mg/m^2), the particle capture rate has reached the transport-limited ceiling, 1.8 mg/m^2 min. These surfaces are extremely adhesive from the biocompatibility perspective. The observed maximum particle deposition rate quantitatively reproduces the calculated pseudo-steady state value (1.81 mg/m^2 min) for deposition/adsorption of a 1-μm Brownian particle/molecule in a slit-shear cell, which is based on the Leveque solution to the convection diffusion equation [60]. At the other extreme, depending on ionic strengths, fibrinogen coverages below about 0.55 mg/m^2 are too low to adhere micron-scale silica particles. Importantly, it appears that small amounts of fibrinogen adsorption can be tolerated before negatively charged micron scale objects begin to foul the surface. Of course, one would expect that surfaces with less dense negative charge than silica, when contaminated with small amounts of fibrinogen, will become adhesive at lower fibrinogen coverages.

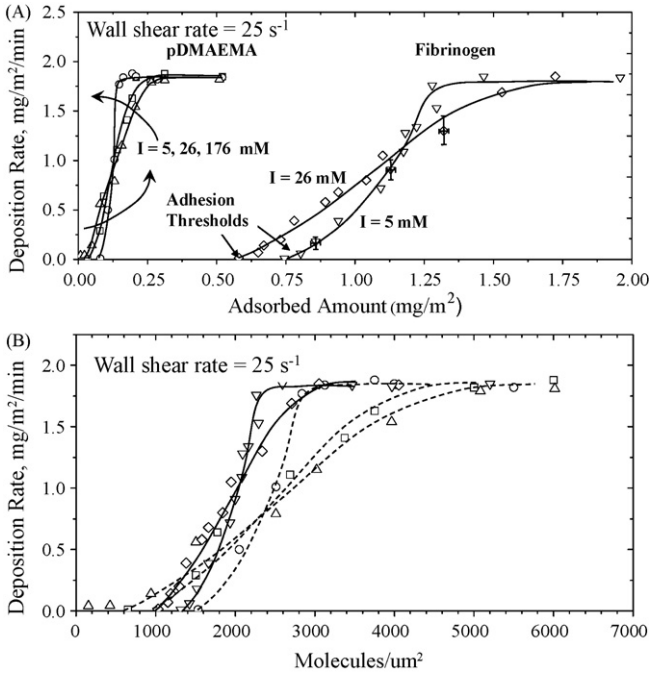

Fig. 6. (A) Adhesion rates of 1 μm silica spheres on silica flats carrying different amounts of adsorbed fibrinogen or pDMAEMA. Different ionic strengths during particle capture are indicated. Data are the average of 2–3 runs, with typical error bars indicated. (B) Data from Part A, with the *x*-axis represented on a molecular rather than mass basis. pDMAEMA data are the dotted lines, fibrinogen is solid. In the fibrinogen studies, diamonds indicate $I = 0.026$ M, while upside down triangles indicate $I = 0.005$ M. In the pDMAEMA studies, circles indicate $I = 0.176$ M, squares indicate $I = 0.026$ M, and circles indicate $I = 0.005$ M.

The capture of 1-μm particles on these fibrinogen-containing surfaces exhibits an adhesion threshold, a coverage of fibrinogen below which silica particles do not adhere. The adhesion threshold indicates that multiple fibrinogen molecules are involved in the capture of each microparticle. This interpretation becomes evident if one considers the opposite extreme, a situation where the data pass through the origin, rather than exhibiting the finite *x*-intercept. If data intersect the origin, then a surface containing any amount of fibrinogen, no matter how small, would be able to capture flowing microparticles. In the extreme, a surface that carried only a single adsorbed fibrinogen molecule would be able to capture one flowing microparticle at an infinitely small rate. Our observation of a positive *x*-intercept (adhesion threshold) therefore reveals that multiple adhesive molecules are involved in the capture of each microparticle. This is sometimes referred to as multi-valent binding or particle capture.

The impact of ionic strength on fibrinogen-mediated particle capture is consistent with the explanation of multi-valent particle binding in the previous paragraph, combined with the previously confirmed [35] random arrangement of fibrinogen on the substrate. First, it is seen in Fig. 6 that the threshold shifts rightward to higher adsorbed amounts of fibrinogen as the ionic strength is reduced. The reason for this is made clear in Fig. 7, which illustrates a particle

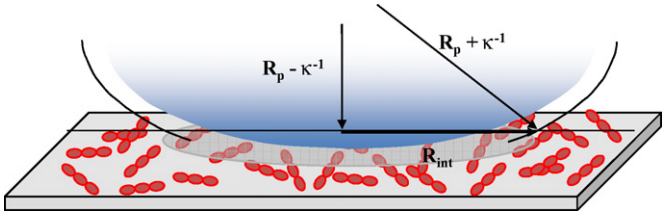

Fig. 7. The radius of the electrostatically interactive area between a planar substrate and a sphere.

interacting with a planar surface. When the repulsive component of the interaction is electrostatic, the amount of planar surface that exerts force on the particle is given by the intersection of a Debye shell around the particle with the planar surface itself. From right triangles, one derives $R_{int} = 2(R_p\kappa^{-1})^{1/2}$, with R_p the particle radius. For $I = 0.005$ and 0.026 M (with $R_p = 0.5$ μm), $R_{int} = 89.4$ and 63.2 nm, respectively. These values are considerably smaller than the microparticles themselves. Particles will be captured when sufficiently large numbers of fibrinogen molecules are present within this interactive area, for a particular position of the particle near the surface. Since the fibrinogen is randomly distributed, some regions of the surface will be more adhesive than others. When R_{int} is relatively small, at high ionic strengths or for small particles/cells, the particle–surface interaction is highly susceptible to particle adhesion on 'hot spots' which contain above-average local fibrinogen concentrations. When R_{int} is large (at low ionic strength or for large particles/cells), the particle sees a more average surface character, which is net negative (per the zeta potentials of Fig. 2). Therefore, conditions with large R_{int} require greater loadings of attractive molecules such as fibrinogen for particle capture.

Included in Fig. 6A are data for surfaces containing small amounts of pDMAEMA rather than fibrinogen. These data, which lie to the left side of the graph, demonstrate that adsorbed pDMAEMA coils capture silica spheres in a manner similar to the action of fibrinogen, although the data are shifted so microsphere capture by pDMAEMA occurs at lower surfaces masses relative to the adsorbed amounts of fibrinogen needed for particle capture. The comparison is a useful one because of our prior studies with pDMAEMA, albeit at pH 6.1 rather than 7.4, render it a well-understood system [41,50,51,53]. It was shown how silica microparticle adhesion is controlled by action of the electrostatically attractive pDMAEMA patches (11 nm in diameter, positively charged, lying flat to the surface) in a background field that is electrostatically repulsive. The pDMAEMA data in Fig. 6 at pH 7.4 are similar to the prior studies at pH 6 with a few small differences. At pH 7.4 in this paper, the silica is more negative than at pH 6. Also, in the current work at pH 7.4, the pDMAEMA carries slightly less positive charge (in Fig. 4) than it did at pH 6 [54].

With the pDMAEMA–silica system of Fig. 6, an adhesion threshold shifts in the same manner with ionic strength as was observed for fibrinogen; however, the threshold and indeed the entire data sets occur at much lower pDMAEMA coverages, in units of mg/m^2. This is because pDMAEMA is a lower molecular weight molecule whose surface saturation, at pH 7.4 and an ionic strength of 0.026 M occurs near 0.5 mg/m^2. Also, as shown in Figs. 2 and 4, only small amounts of pDMAEMA are needed to alter the silica zeta potential compared with the amounts of adsorbed fibrinogen. Returning back to Fig. 6, variations in ionic strength cause the fibrinogen and pDMAEMA data sets each to cross. We previously demonstrated that the crossing is a result of the random placement of adhesive elements, and the coverage where the crossing occurs gives an estimate of the local concentration of adhesive elements within the interactive radius, required for adhesion [53]. The series with pDMAEMA also contains data in $I = 0.176$ M phosphate-buffered saline, which continues the trend of ionic strength, further upholding the arguments concerning the impact of Debye length on the interactive area, convoluted with the statistics of random "sticker" placement.

Fig. 6B renormalizes the x-axis of Fig. 6A so that fibrinogen-containing and pDMAEMA-containing surfaces can be more directly compared. If one considers the average numbers of molecules per unit area on the silica, rather than the adsorbed mass, one finds quantitatively similar (though not identical behavior) results for microparticle capture rates. This suggests that each fibrinogen or pDMAEMA molecule contributes nearly the same attractive energy towards approaching silica spheres, and also that roughly the same numbers of pDMAEMA or fibrinogen molecules are locally involved in the capture of each microparticle.

Simulated particle capture data at pH 6.1, where the silica background charge is weaker and the pDMAEMA patches are more positively charged compared with the current study, reveal the exact numbers of pDMAEMA patches involved in microparticle capture [53]. These prior results set a lower bound on the number of molecules involved in microparticle capture in the current study: at an ionic strength of 0.005 M corresponding to a Debye length, κ^{-1}, of 4.2 nm, at least 40 pDMAEMA patches were needed to capture each microparticle. At $I = 0.026$ M ($\kappa^{-1} = 2.0$ nm) the figure was 20 pDMAEMA patches. And for $\kappa^{-1} = 1$ nm, 10 patches were needed. We expect, greater numbers of polymer coils/proteins, to be involved in the capture of each microparticle in the current work, but these figures should be the same order of magnitude.

An important difference between pDMAEMA and fibrinogen is that pDMAEMA is positively charged at pH 7.4 while fibrinogen is net negative. When the molecules adsorb on silica at low concentrations, Fig. 2 suggests that the electrostatic environment around the pDMAEMA patches is slightly positive while around the adsorbed fibrinogen it is still net negative, approaching neutrality at higher ionic strengths. The observation of the similar adhesion rate signatures in Fig. 6B suggests, however, similar mechanisms for particle adhesion: adsorbed fibrinogen molecules act as distinct adhesive elements with net attraction towards approaching microparticles. In the case of pDMAEMA the attractions were a combination electrostatic and van der Waals interactions, with the latter dominated by the underlying silica. In the case of fibrinogen, the attractions may result from a combination of electrostatics, hydrophobicity, and donor-acceptor interactions such as hydrogen bonding, in addition to van der Waals interactions. Interestingly, though the fibrinogen is net negatively charged, its positive central domain may be accessible when it is adsorbed, and may dominate the negative regions of the molecule.

3.3. Fibrinogen in physiological buffer

When silica microparticles were flowed over fibrinogen-containing silica surfaces in $I = 0.176$ M phosphate-buffered saline, no particle capture was seen at any fibrinogen loading. This was the case even for saturated fibrinogen layers, near 2.0 mg/m^2. Thus these ionic conditions appear to be ones where fibrinogen is modestly attractive to silica (enough so to adsorb in Fig. 1), but once adsorbed, it is not substantially attractive towards gently flowing silica microspheres. This apparent paradox speaks to the conformation of the adsorbed fibrinogen. It may be the case that not all faces of the fibrinogen molecule are equally attracted to silica, and fibrinogen adsorbs with a silica-philic face preferentially towards the silica flat. Thus when the ionic strength is raised, the outward facing portion of the molecule has weaker interactions with new silica surfaces than the face of the fibrinogen which had originally adsorbed.

A number of control runs were conducted to reinforce this result: first, a TIRF experiment employing fluorescently tagged fibrinogen revealed that flowing silica microparticles did not remove fibrinogen from the substrate at these ionic conditions. Second, for a fibrinogen coverage of 2.0 mg/m^2 corresponding to saturation in 0.176 M buffered saline, there was no silica particle capture at an ionic strength of 0.176 M. However, in a continuation of this run, reversal of the ionic strength back to 0.026 or 0.005 M enabled rapid transport-limited silica particle capture, as reported in Fig. 6. This demonstrates that the impact of ionic strength on the ability of adsorbed fibrinogen to adhere additional silica particles is reversible with changes in ionic strength, and likely is a direct result of immediate fibrinogen–silica and silica–silica interactions, rather than slower protein reconformations. (The time course of changing the ionic conditions was a few minutes.)

The observation that adsorbed fibrinogen does not capture silica particles at physiological ionic strength is surprising. While we have demonstrated that the affinity of fibrinogen for silica is reduced at the high ionic strength compared with its adsorption at low ionic strength, fibrinogen attraction to silica in the $I = 0.176$ M buffer is far from eliminated. Indeed, Fig. 2 shows that saturated layers of fibrinogen on silica (or silica surfaces carrying greater than 0.5 mg/m^2) are nearly net neutral at the ionic strength of 0.176 M, while there is a substantial net negative character to the same surfaces at lower ionic strengths. Therefore, from the perspective of average surface properties, higher ionic strengths should favor particle adhesion by making the relative contributions of van der Waals attractions more important than electrostatic repulsions. (The ability of pDMAEMA patches to capture silica spheres at high ionic strengths in Fig. 6 reinforces this point.) Therefore, the stabilizing mechanism that prevents fibrinogen from capturing the microspheres at high ionic strengths could be screening of the electrostatic attractions between positive regions of fibrinogen and the negative silica particles. Screened attractions involving electrostatically heterogeneous surfaces has been proposed to explain the reduced adhesion of some bacteria at elevated ionic strengths [25], and we have quantitatively demonstrated the range of heterogeneities where ionic strength reduces versus increases net attractions [53].

Alternatively, there exist reports of the influence of hydration forces on protein–surface interactions, suggesting that hydration forces at elevated salt concentrations contribute to the inability of adsorbed fibrinogen to capture negative microparticles. For instance, Tsapikouni et al. find diminished attractions between fibrinogen-coated silica spheres and mica flats in their atomic force microscopy studies at elevated (0.5 M) salt concentrations, and attribute the effect to hydration of Na^+ ions [61,62], which were previously shown to be trapped at high concentrations on negative surfaces [63]. Molina-Bolivar and Ortega-Vinuesa also argue for the stabilizing effects of hydration forces from adsorbed proteins on colloidal stability [64].

4. Summary and conclusions

This study demonstrated how small amounts of fibrinogen adsorbed onto negatively charged surfaces can facilitate capture of micron-sized particles, overcoming the net negative surface character which includes the adsorbed fibrinogen molecules themselves. As the silica surfaces used in this study are among the most densely negatively charged surfaces that one might encounter in biomaterial and diagnostic applications, the 0.5 mg/m^2 fibrinogen thresholds that produced adhesion of silica microspheres represent an upper bound on the amount of adsorbed protein that can lead to surface fouling by cells and other particulates. This figure could be used as a quantitative guideline for the assessment of "protein resistance" and "biocompatibility", terms which are employed broadly to materials whose protein resistance may not be sufficient to avoid cell adhesion.

A related observation was that no silica particle adhesion was found to occur below the adhesion threshold of fibrinogen: for fibrinogen loadings below about 0.5 mg/m^2, the microparticles were stabilized against adhesion by electrostatic repulsion. The observation of the threshold, with a complete lack of particle capture at lower fibrinogen loadings, indicated that when particles did adhere (at fibrinogen loadings above 0.5 mg/m^2) they adhered only to regions which contained multiple fibrinogen molecules within a contact radius. This mechanism of particle capture was facilitated by the random arrangement of the adsorbed fibrinogen and the finite probability that some regions of the surface contained above-average local fibrinogen concentrations. These conclusions are supported by the similar behavior of silica particle capture by small levels of cationic polymer. Though the fibrinogen molecules are generally negative (contrasted with the positive charge of the cationic pDMAEMA coils), the comparison illustrates how particle capture is affected by ionic strength when the repulsive component of the interaction is electrostatic. Comparison to the electrostatic system allowed us to place a lower bound on the numbers of fibrinogen involved in microsphere capture, order 10–40 for the range of ionic strengths studied.

Acknowledgements

This work was made possible by NSF grants CBET-0428455 and BMAT-0805061, and aid from the UMass-Baystate initiative.

References

[1] M. Herrmann, P.E. Vaudaux, D. Pittet, R. Auckenthaler, P.D. Lew, F. Schumacher-perdreau, G. Peters, F.A. Waldvogel, Journal of Infectious Diseases 158 (1988) 693–701.
[2] P. Vaudaux, D. Pittet, A. Haeberli, E. Huggler, U.E. Nydegger, D.P. Lew, F.A. Waldvogel, Journal of Infectious Diseases 160 (1989) 865–875.
[3] P. Toy, L.W. Lai, T.A. Drake, M.A. Sande, Infection and Immunity 48 (1985) 83–86.
[4] P. Vaudaux, R. Suzuki, F.A. Waldvogel, J.J. Morgenthaler, U.E. Nydegger, Journal of Infectious Diseases 150 (1984) 546–553.
[5] P.E. Vaudaux, F.A. Waldvogel, J.J. Morgenthaler, U.E. Nydegger, Infection and Immunity 45 (1984) 768–774.
[6] P. Vaudaux, H. Yasuda, M.I. Velazco, E. Huggler, I. Ratti, F.A. Waldvogel, D.P. Lew, R.A. Proctor, Journal of Biomaterials Applications 5 (1990) 134–153.
[7] P. Francois, J. Schrenzel, C. Stoerman-Chopard, H. Favre, M. Herrmann, T.J. Foster, D.P. Lew, P. Vaudaux, Journal of Laboratory and Clinical Medicine 135 (2000) 32–42.
[8] A.L. Cheung, V.A. Fischetti, Journal of Infectious Diseases 161 (1990) 1177–1186.
[9] D. McDevitt, P. Francois, P. Vaudaux, T.J. Foster, Molecular Microbiology 11 (1994) 237–248.
[10] G.S. Chhatwal, K.T. Preissner, G. Mullerberghaus, H. Blobel, Infection and Immunity 55 (1987) 1878–1883.
[11] O.D. Liang, M. Maccarana, J.I. Flock, M. Paulsson, K.T. Preissner, T. Wadstrom, Biochimica Et Biophysica Acta 1225 (1993) 57–63.
[12] M. Herrmann, S.J. Suchard, L.A. Boxer, F.A. Waldvogel, P.D. Lew, Infection and Immunity 59 (1991) 279–288.
[13] M. Herrmann, J. Hartleib, B. Kehrel, R.R. Montgomery, J.J. Sixma, G. Peters, Journal of Infectious Diseases 176 (1997) 984–991.
[14] P. Francois, P. Vaudaux, T.J. Foster, P.D. Lew, Medecine Et Maladies Infectieuses 27 (1997) 143–149.
[15] R.B. Dickinson, J.A. Nagel, D. McDevitt, T.J. Foster, R.A. Proctor, S.L. Couper, Infection and Immunity 63 (1995) 3143–3150.
[16] R.B. Dickinson, Journal of Colloid and Interface Science 190 (1997) 142–151.
[17] H.L. Ma, R.B. Dickinson, Journal of Theoretical Biology 226 (2004) 237–250.
[18] E. Evans, Annual Review of Biophysics and Biomolecular Structure 30 (2001) 105–128.
[19] E. Evans, Faraday Discussions (1998) 1–16.
[20] R. Merkel, P. Nassoy, A. Leung, K. Ritchie, E. Evans, Nature 397 (1999) 50–53.
[21] Y. Liu, J. Strauss, T.A. Camesano, Biomaterials 29 (2008) 4374–4382.
[22] H.J. Busscher, W. Norde, H.C. Van der Mei, Applied and Environmental Microbiology 74 (2008) 2559–2564.
[23] D.H. Kim, A.L. Klibanov, D. Needham, Langmuir 16 (2000) 2808–2817.
[24] D.A. NopplSimson, D. Needham, Biophysical Journal 70 (1996) 1391–1401.
[25] H.J. Busscher, B. van de Belt-Gritter, R.J.B. Dijkstra, W. Norde, H.C. van der Mei, Langmuir 24 (2008) 10968–10973.
[26] C.P. Xu, B. van de Belt-Gritter, R.J.B. Dijkstra, W. Norde, H.C. van der Mei, H.J. Busscher, Langmuir 23 (2007) 9423–9428.
[27] A. Roosjen, H.C. van der Mei, H.J. Busscher, W. Norde, Langmuir 20 (2004) 10949–10955.
[28] K. Vacheethasanee, J.S. Temenoff, J.M. Higashi, A. Gary, J.M. Anderson, R. Bayston, R.E. Marchant, Journal of Biomedical Materials Research 42 (1998) 425–432.
[29] S.F. Chen, J. Zheng, L.Y. Li, S.Y. Jiang, Journal of the American Chemical Society 127 (2005) 14473–14478.
[30] N.P. Huang, R. Michel, J. Voros, M. Textor, R. Hofer, A. Rossi, D.L. Elbert, J.A. Hubbell, N.D. Spencer, Langmuir 17 (2001) 489–498.
[31] G.L. Kenausis, J. Voros, D.L. Elbert, N.P. Huang, R. Hofer, L. Ruiz-Taylor, M. Textor, J.A. Hubbell, N.D. Spencer, Journal of Physical Chemistry B 104 (2000) 3298–3309.
[32] L. Andruzzi, W. Senaratne, A. Hexemer, E.D. Sheets, B. Ilic, E.J. Kramer, B. Baird, C.K. Ober, Langmuir 21 (2005) 2495–2504.
[33] B. Zdyrko, P.B.Y. Ofir, A.M. Alb, W.F. Reed, M.M. Santore, Journal of Colloid and Interface Science 322 (2008) 365–374.
[34] Y.A. Que, J.A. Haefliger, L. Piroth, P. Francois, E. Widmer, J.M. Entenza, B. Sinha, M. Herrmann, P. Francioli, P. Vaudaux, P. Moreillon, Journal of Experimental Medicine 201 (2005) 1627–1635.
[35] A. Toscano, M.M. Santore, Langmuir 22 (2006) 2588–2597.

[36] L. Feng, J.D. Andrade, in: T.A. Horbett, J.L. Brash (Eds.), Proteins at Interfaces II: Fundamentals and Applications, 602, American Chemical Society, Washington, DC, 1994, pp. 66–79.
[37] C.F. Wertz, M.M. Santore, Langmuir 18 (2002) 706–715.
[38] H.J. Kim, E.L.M. Gias, M.N. Jones, Colloids and Surfaces A-Physicochemical and Engineering Aspects 149 (1999) 561–570.
[39] G.M. Bruinsma, M. Rustema-Abbing, H.C. van der Mei, H.J. Busscher, Journal of Microbiological Methods 45 (2001) 95–101.
[40] J.F.L. Duval, H.J. Busscher, B. van de Belt-Gritter, H.C. van der Mei, W. Norde, Langmuir 21 (2005) 11268–11282.
[41] S. Kalasin, M.M. Santore, Langmuir 24 (2008) 4435–4438.
[42] N. Mohamed, T.R. Rainier, J.M. Ross, Biotechnology and Bioengineering 68 (2000) 628–636.
[43] S.L. Walker, J.A. Redman, M. Elimelech, Langmuir 20 (2004) 7736–7746.
[44] S.L. Walker, J.A. Redman, M. Elimelech, Environmental Science & Technology 39 (2005) 6405–6411.
[45] V.A. Rebar, M.M. Santore, Journal of Colloid and Interface Science 178 (1996) 29–41.
[46] C.T. Shibata, A.M. Lenhoff, Journal of Colloid and Interface Science 148 (1992) 485–507.
[47] C.F. Wertz, M.M. Santore, Langmuir 15 (1999) 8884–8894.
[48] M.M. Santore, C.F. Wertz, Langmuir 21 (2005) 10172–10178.
[49] C.F. Wertz, M.M. Santore, Langmuir 17 (2001) 3006–3016.
[50] N. Kozlova, M.M. Santore, Langmuir 22 (2006) 1135–1142.
[51] M.M. Santore, N. Kozlova, Langmuir 23 (2007) 4782–4791.
[52] Z.G. Fu, M.M. Santore, Colloids and Surfaces A-Physicochemical and Engineering Aspects 135 (1998) 63–75.
[53] R. Duffadar, S. Kalasin, J.M. Davis, M.M. Santore, Journal of Colloid and Interface Science, (2009), doi:10.1016/j.jcis.2009.05.046.
[54] Y.W. Shin, J.E. Roberts, M.M. Santore, Journal of Colloid and Interface Science 247 (2002) 220–230.
[55] Y. Shin, J.E. Roberts, M.M. Santore, Macromolecules 35 (2002) 4090–4095.
[56] N. Hansupalak, M.M. Santore, Macromolecules 37 (2004) 1621–1629.
[57] N. Hansupalak, M.M. Santore, Langmuir 19 (2003) 7423–7426.
[58] M.M. Santore, Current Opinion in Colloid & Interface Science 10 (2005) 176–183.
[59] G.J. Fleer, M.A. Cohen Stuart, J.M.H.M. Scheutjens, T. Cosgrove, B. Vincent, Polymers at Interfaces, Chapman and Hall, London, 1993.
[60] M.A. Leveque, Annales Des Mines 13 (1928) 284.
[61] T.S. Tsapikouni, S. Allen, Y.F. Missirlis, Biointerphases 3 (2008) 1–8.
[62] T.S. Tsapikouni, Y.F. Missirlis, Colloids and Surfaces B-Biointerfaces 57 (2007) 89–96.
[63] R.M. Pashley, Journal of Colloid and Interface Science 83 (1981) 531–546.
[64] J.A. Molina-Bolivar, J.L. Ortega-Vinuesa, Langmuir 15 (1999) 2644–2653.